Zoodiversity, 60(2): 163–178, 2026

DOI 10.15407/zoo2026.02.163
UDC: 599.32(477)

SPATIAL DISTRIBUTION MODELLING OF *STYLODIPUS TELUM FALZFEINI* (RODENTIA, DIPODIDAE) IN THE OLESHKY SANDS USING MAXENT AND LANDSAT REMOTE SENSING DATA

Yu. Moskalenko

Black Sea Biosphere Reserve, NAS of Ukraine, Lermontova st., 1, Hola Prystan, Kherson Reg., 75600 Ukraine

E-mail: strix@strix.ks.ua

Yu. O. Moskalenko (https://orcid.org/0000-0002-9121-7832)

urn:lsid:zoobank.org:pub:8CE354C0-55CB-49CE-A347-FAC4624AF43F

Spatial distribution modelling of *Stylodipus telum falzfeini* (Rodentia, Dipodidae) in the Oleshky Sands using Maxent and Landsat remote sensing data. Moskalenko, Yu. O. — The aim of this study was to model the spatial distribution of the endemic subspecies of the thick-tailed three-toed jerboa *Stylodipus telum falzfeini* (Brauner, 1913) within the Oleshky Sands using remote sensing data and the Maxent software. The modelling was based on occurrence data from 440 *S. t. falzfeini* burrows. The components of the Tasselled Cap Transformation derived from Landsat-8 remote sensing data were used as ecogeographical variables. The results demonstrated that the selected satellite-derived metrics are well-suited for modelling the spatial distribution of the jerboa. The habitat suitability map revealed that three-fifths of the Oleshky Sands are completely unsuitable for this subspecies. In most arenas, this figure ranges from 55.3% to 65.6%, reaching 80.8% on the Kinburn Peninsula and 78.4% in the Kakhovska arena. As for suitable habitats, not only do they represent a relatively small proportion of the landscape, but they are also highly fragmented due to afforestation efforts, during which extensive areas of pine plantations were established across the Oleshky Sands. The successful modelling of the jerboa's distribution using temporally comparable satellite-derived metrics enables retrospective analysis of distributional changes within the Oleshky Sands and subsequent detailed assessment of the factors that have influenced these changes over recent decades. Moreover, the data obtained capture the pre-war state of the jerboa population and may serve in future as a baseline for assessing the impacts of the war on this population.

Key words: species distribution models, Dipodidae, habitat fragmentation, Oleshky Sands, remote sensing data, Tasseled Cap Transformation, Maxent.

Introduction

The main range of the Thick-Tailed Three-Toed Jerboa (*Stylodipus telum* (Lichtenstein, 1823)) covers deserts, semi-deserts and southern steppes, stretching from the Volga-Don divide in the west to the left bank of the middle reaches of Irtysh River in the east (Gromov & Baranova, 1981). In Ukraine, in an isolated part of this species range, it is represented by a subspecies *Stylodipus telum falzfeini* (Brauner, 1913) (Shenbrot et al., 1995). The latter is a narrowly distributed endemic, occurring only in the Oleshky Sands (OS), which area is less than 2,000 km^2. The economic development of the OS negatively affected the population of *S. t. falzfeini*, and since 1980 the jerboa has been given a protected status (Red Data…, 1980; Hyzenko, 1985; Red Data…, 1994, 2009).

The main factor negatively affecting the *S. t. falzfeini* population is the destruction of this subspecies' habitats within the OS due to the establishment of artificial forest plantations (Hyzenko 1985; Selyunina 1995). Therefore, to conserve *S. t. falzfeini*, it was proposed to grant protected status to the unforested areas of the OS (Red Data…, 2009). An important step in this direction was the establishment of the Oleshky Sands National Nature Park in 2010, covering an area of 8,020.36 ha, followed by its expansion by a further 3,650.7 ha in 2019 (Ministry…, 2020).

As a result of the large-scale invasion by Russian armed forces on 24 February 2022, the entire territory of the OS came under occupation. This has created new threats to the conservation of the *S. t. falzfeini* population, as the war not only makes any conservation practices impossible but also exerts a significant destabilising impact on natural ecosystems (Zagorodniuk, 2023). Almost from the very beginning of the full-scale invasion, some parts of the OS, particularly the Kinburn Peninsula and Ivanivska Arena, became sites of active hostilities. Following the retreat of Russian occupying forces from the right-bank part of the Kherson region, combat activities to varying extents have affected nearly the entire territory of the OS. As a result, its ecosystems have suffered due to large-scale fires, the construction of fortifications, and other war-related disturbances. The coastal areas of the sand massifs were also impacted by temporary flooding caused by the destruction of the Kakhovka Hydroelectric Power Station by Russian occupying forces.

Researchers consider the potential threats posed by military actions to be not only to *S. t. falzfeini*, but also to several other endangered mammal species inhabiting the OS, such as *Spalax arenarius* Reshetnik, 1939 and *Sicista loriger* (Nathusius, 1840) (Rusin, 2023; Zagorodniuk & Korobchenko, 2023; Kolodezhna & Vasyliuk, 2025). In these circumstances, documenting the pre-war distribution of *S. t. falzfeini* is highly relevant, particularly through species distribution modelling, as this provides a basis for comparing the post-war status of the subspecies' population and for developing and implementing conservation measures.

The species distribution modelling (SDM) allows coping with a wide range of tasks, including those associated with the conservation of vulnerable species (Franklin & Miller, 2010; Tytar, 2011). As for *S. t. falzfeini*, the SDM will give a possibility to identify what part of the OS is occupied with its population, to make a retrospective analysis of changes in its distribution and highlight the

main factors influencing it, estimate risks of the population extinction in the study area, plan further monitoring of the population dynamics and to develop conservation measures.

Intending to model the spatial distribution of *S. t. falzfeini* within the OS, we have set the following three objectives:

a) to estimate the feasibility of using remote sensing data (RSD) for the distribution modelling of *S. t. falzfeini* within the OS;

b) to model the habitat suitability map for *S. t. falzfeini* using the selected RSD;

c) to evaluate the size of suitable habitats for *S. t. falzfeini* within the OS.

Material and Methods

Study area. The Oleshky Sands (OS) comprise seven large arenas (Fig. 1), which extend downstream from Kakhovka City along the Dnipro and Dniprovskyi Liman (Gordienko, 1969). The natural landscape of OS is defined as intrazonal hilly-sandy forest-steppe (Tkachenko, 1999). Wood-steppe sections of the Black Sea Biosphere Reserve (Solonoozerna section, Ivano-Rybalchanska section, and Volyzhin Forest section) are the only areas where relatively untouched parts of this landscape can still be found.

In most areas of the OS, large artificial pine plantations with some deciduous species (mainly black locusts, *Robinia pseudoacacia* L.) were established to mitigate sand deflation caused by the destruction of natural vegetation due to excessive grazing and forest cutting. The remaining part of the OS, which was either not forested or lost its artificial pine plantations due to fires, mostly consists of open landscapes with vegetation at different stages of restorative succession.

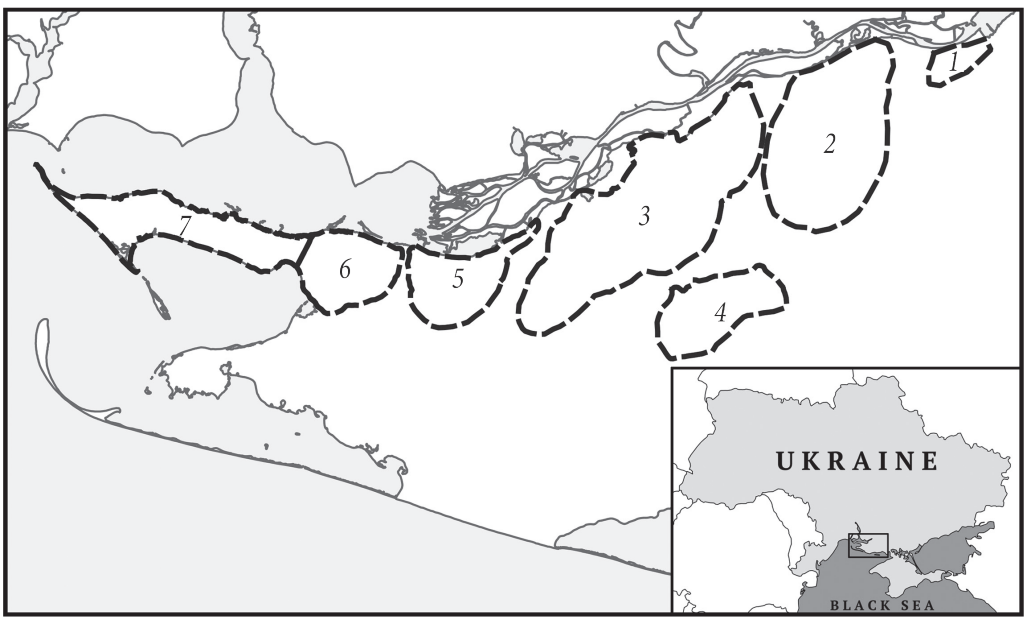

Fig. 1. Study area. Arenas of the OS: *1* — Kakhovska; *2* — Kozachelaherska; *3* — Oleshkyvska; *4* — Chalbaska; *5* — Zburivska; *6* — Ivanivska; *7* — Kinburn Peninsula

Collection and preprocessing of field occurrence data. The field data was collected during 2016–2017 in Kozachelaherska, Oleshkyvska, Zburivska, Ivanivska arenas, and on the Kinbrun Peninsula. During the field trips, we identified the burrows of *S. t. falzfeini* and recorded their GPS coordinates in WGS 1984 coordinate system (EPSG: 4326). A total of 440 burrow coordinates were obtained.

The occurrence points were collected without a specific sampling design, concurrently with other studies. Therefore, using such a dataset for species distribution modelling may result in an overfitted model due to sampling bias and spatial autocorrelation (Boria et al., 2014; Aiello-Lammens et al., 2015). In such cases, spatial filtration is typically employed to reduce sample bias and spatial autocorrelation (Boria et al., 2014). First, we split the full dataset into two parts. The first subset, which was used to form an independent sample for evaluating the predictive performance of the models under spatial extrapolation, included all occurrence records from the Zburivska arena (141 points in total). The Zburivska arena was selected for the independent sample because occurrence records there were collected across its various parts, encompassing markedly different environmental conditions, which made this area a suitable testing ground for evaluating the spatial transferability of the models. The second subset (comprising 299 points in total) was used to form the calibration dataset. Both the calibration dataset and the dataset for evaluating the spatial transferability of the models were generated by applying spatial thinning using the "thin" function from the R package spThin (version 0.2.0), which returns a random subsample with the maximum number of occurrence records for a specified thinning distance (Aiello-Lammens et al., 2015). The minimum distance between occurrence records was set at 0.5 km, resulting in a samples of 81 points (for model calibration purpose) and of 38 points (for evaluating the spatial transferability of the models).

Before using the occurrence data, we reprojected its coordinates to the local coordinate system (UTM36N; EPSG 32636), which matches the coordinate system used in the RSD in our research.

Predictor variables selection. The maximum length of the OS is about 150 km, so our study corresponds to the landscape scale domain. According to Pearson & Dawson (2003) and Araújo et al. (2019), habitat characteristics such as topography, vegetation parameters, soil type, and others have a dominant control over species distributions at this scale. Creating maps of habitat characteristics at a sufficient resolution for species distribution modelling at a landscape scale is often challenging or even impossible due to the difficulty of directly measuring habitat variables. Moreover, mapped habitat variables may not accurately capture ecologically meaningful functional variability for a species (Leyequien et al., 2007). Consequently, an indirect approach using RSD and its derivative products as proxies for habitat characteristics has become widespread in species distribution modelling (Leyequien et al., 2007).

Many habitat variables can be assessed through RSD. For example, vegetation fractional cover is closely correlated with the values of certain spectral indices computed from RSD (Todd & Hoffer, 1998; Gitelson et al., 2002). Other RSD-derived products can serve as proxies for soil variability, moisture content in soil and vegetation, and topographic factors such as elevation, slope, and aspect (Bertoldi et al., 2010; Li et al., 2013; Roberts et al., 2015). These findings suggest that RSD can be

effectively used as a proxy for modelling the spatial distribution of *S. t. falzfeini* within the OS at a landscape scale.

The key criteria we used in selecting variables was their suitability for constructing a model that could be projected to past or future years. This is necessary for further research on the retrospective dynamics of *S. t. falzfeini* habitats, as well as for monitoring their future changes. Therefore, in the initial stages of our study, we decided to exclude raw RSD spectral bands just as vegetation indices from potential proxies due to their high intercorrelation, which can result in the problem of multicollinearity. Although the Maxent SDM is robust to multicollinearity among predictor variables during model calibration, multicollinearity can negatively affect model transferability in space or time (Simoes et al., 2020).

Of course, the issue of multicollinearity can be solved through PCA, but models based on principal components cannot be projected in time as it is not feasible to compare the principal components obtained from one scene of RSD with those obtained from another scene of RSD. A more appropriate approach for addressing the issue of intercorrelation between spectral bands in our study was the use of Tasseled Cap Transformation (TCT). This transformation converts the RSD spectral bands into new orthogonal components where most of the data variance is concentrated in the first three components, namely Tasseled Cap Brightness (TCB), Tasseled Cap Greenness (TCG), and Tasseled Cap Wetness (TCW) (Vorovencii, 2007). TCB is a quantitative measure of the total land surface reflectivity, while TCG intensity characterizes the density of green vegetation, and TCW characterizes the moisture content of the soil and vegetation (Chandra & Ghosh, 2007). Unlike PCA, the TCT produces directly comparable invariant features, for example between scenes or sensors (Vorovencii, 2007). Thanks to this property, SDMs based on TCT components can be projected in space or time.

Obtaining and preparation RSD. In this study, we used RSD acquired by the on-board Operational Land Imager (OLI) instrument of Landsat 8. We selected cloud-free Landsat 8 RSD scenes acquired on 30 August 2015 (scene IDs: LC81790272015242LGN01 and LC81790282015242LGN01), 15 July 2016 (LC81790272016197LGN01 and LC81790282016197LGN01), 29 April 2017 (LC81790272017119LGN00 and LC81790282017119LGN00), and 31 May 2017 (LC81790272017151LGN00 and LC81790282017151LGN00). The final selection of which of these scenes were to be used in the modelling process was made during model calibration.

Initial steps of RSD preparation were carried out in the Google Earth Engine environment, a cloud-based platform for geospatial analysis and computation (Gorelick et al., 2017). These steps included selecting the required Landsat 8 RSD scenes from the USGS Landsat 8 Collection 2 Tier 1 TOA Reflectance dataset, mosaicking adjacent scenes covering the study region, computing the TCT components (i. e., TCB, TCG and TCW) according to the coefficients developed by Baig et al. (2014), applying a 5 × 5 pixel median filter to reduce high-frequency noise, cropping the layers to match the region of interest, and exporting the resulting products as GeoTIFF raster files.

Subsequently, the 'gdalwarp' utility from the GDAL software package (GDAL/OGR contributors, 2017) was used together with a shapefile delineating the OS

boundaries to mask out areas outside the arenas in each raster layer. This step was necessary to ensure that the entire habitat suitability modelling workflow in Maxent — including the generation of background points — was restricted strictly to within the OS boundaries.

In the final step, the obtained covariates were converted from GeoTIFF to raster Arc/Info ASCII Grid format using the 'gdal_translate' utility from the GDAL software package.

The source code of the scripts implementing these RSD preparation steps is publicly available in a Zenodo repository (see Supplementary materials section for details).

Model calibration, fitting, and evaluation. To model the habitat suitability of *S. t. falzfeini*, we used Maxent software version 3.4.4 (Phillips et al., 2006; Phillips et al., 2017). Optimal model parameters, including the regularisation multiplier value, the feature class combination (linear — L, quadratic — Q, hinge — H, product — P, and threshold — T), and the RSD, were selected by calibrating the model using the 'kuenm' R package, which automates key calibration procedures (Cobos et al., 2019). Following Simoes et al. (2020), model performance during calibration was assessed based on three criteria in the following order: statistical significance (partial ROC), predictive ability (omission rates < 5%), and model complexity (AICc — Akaike's Information Criterion corrected for small sample sizes). The final decision to accept or reject a model was made based on a predictive ability test using an independent dataset — a model was considered acceptable if the omission rate in this test was less than 5%.

During parameter tuning, the calibration dataset was randomly split into training (80%) and testing (20%) subsets for model performance evaluation. In both the calibration phase and the development of the final model, the number of randomly generated background points was set to 30,000.

The final model was fitted using a total of 119 occurrence points (i. e., combined calibration and testing subsets), based on 30 Maxent bootstrap replicates, with model parameters and the RSD dataset as selected during the calibration process. To evaluate the performance of the final model and to assess the contributions of the predictor variables, 20% of the occurrence points were allocated as a test subsample.

Results

Optimal parameters for model training were selected after several iterations of calibration, performed using the 'kuenm' package. During the initial iterations, we evaluated sets of models based on individual feature classes (L, Q, H, P, and T) and all their possible pairwise combinations, using all four sets of TCT components. Following these evaluations, the threshold feature was discarded due to signs of overfitting: although models including this feature showed good performance on training and testing datasets, omission rates on the independent dataset were excessively high. For the same reason, the TCT component set from 30 August 2015 was excluded. During the final iteration of calibration, we evaluated 480 candidate models encompassing all possible combinations of 16 regularisation multiplier values (0.1, 0.2,

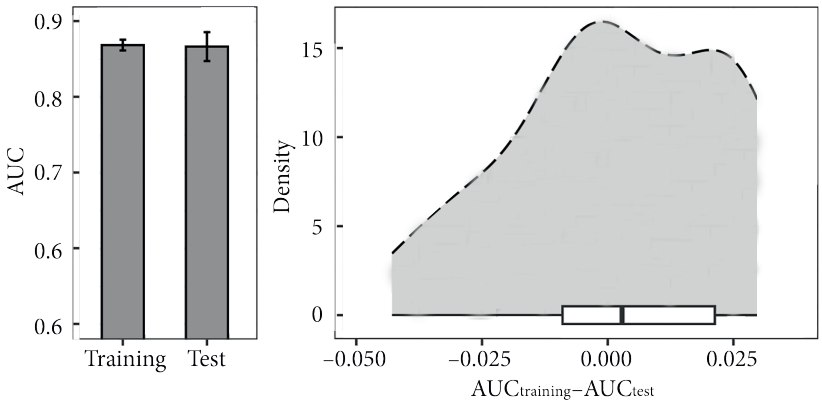

a *b*

Fig. 2. Model evaluation results based on AUC: *a*) Barplot showing training and test AUC (mean of 30 runs shown as bars with ±1 SD error bars); *b*) Density plot and boxplot visualizing the distribution of the differences between training and test AUC values

0.3, 0.4, 0.5, 0.6, 0.7, 0.8, 0.9, 1, 2, 3, 4, 5, 6, 7), 10 feature class combinations (L, Q, P, H, QP, LQ, LP, LH, QH, PH), and 3 sets of TCT components (Set 2 — 15 July 2016; Set 3 — 29 April 2017; and Set 4 — 31 May 2017). All candidate models were found to be statistically significant. Of these, 332 models exhibited an omission rate of less than 0.05, and three also met the AICc criterion (ΔAICc <= 2), as detailed in Table 1. Evaluation of these three models on the independent dataset demonstrated their good performance (Table 2). The calibration parameters from candidate model #1, which had the lowest AICc value, were selected for building the final model.

Table 1. **Calibration parameters and performance statistics for candidate models meeting all selection criteria**

Candidate model	Combination of the calibration parameters	Mean AUC ratio	Partial ROC (*p*-value)	Omission rate at 5%	AICc	Delta AICc	W AICc	No. Parameters
1	M: 0.3; F: LQ; Set2	1.645	0.000	0	2190.110	0.000	0.158	4
2	M: 0.4; F: LQ; Set2	1.645	0.000	0	2190.297	0.188	0.144	4
3	M: 0.2; F: LQ; Set2	1.644	0.000	0	2192.119	2.009	0.058	5

Note. M — regularisation multiplier value; F — feature class combination; Set2 — TCT components calculated from remote sensing data acquired on 15 July 2016.

Table 2. **Evaluation results of candidate models based on the independent dataset**

Candidate model	Combination of the calibration parameters	Mean AUC ratio	Partial ROC (*p*-value)	Omission rate at 5%
1	M: 0.3; F: LQ; Set2	1.593	0	0.036
2	M: 0.4; F: LQ; Set2	1.593	0	0.036
3	M: 0.2; F: LQ; Set2	1.570	0	0.036

The final model of habitat suitability for *S. t. falzfeini* exhibits relatively high AUC values, with a training AUC of 0.869 (SD = 0.007) and a test AUC of 0.867 (SD = 0.019) (Fig. 2, *a*). According to the AUC value range scale provided by Araújo et al. (2005), the model demonstrates good predictive accuracy. Furthermore, only a small difference between the training and test AUC values was observed (Fig. 2, *b*). As noted by Abdelaal et al. (2019), this suggests the absence of substantial overfitting.

The averaged response curves generated from the 30 Maxent runs during the construction of the final model exhibit a classical unimodal, bell-shaped pattern (Fig. 3). However, the curves for TCB and TCW appear truncated (on the right for TCB and on the left for TCW), which indicates that completely unsuitable conditions for *S. t. falzfeini* occur only at one end of the gradients of these variables.

In the final model, TCW exhibited the highest significance in the permutation tests, followed by TCG, while TCB showed the lowest permutation importance (Fig. 4, *a*). Considering the estimates of the relative contributions of the environmental variables, TCW received the highest score, whereas the contributions of TSG and, particularly, TSB were low (Fig. 4, *b*).

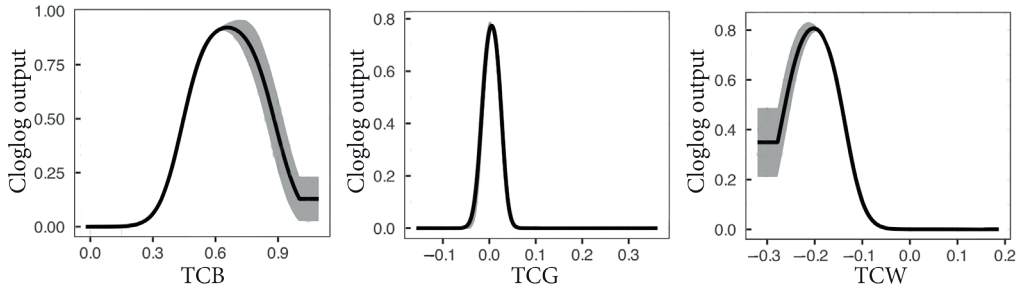

Fig. 3. Response curves of environmental variables in the Maxent potential habitat suitability model for *S. t. falzfeini* (mean of 30 runs in black, ± 1 SD in grey)

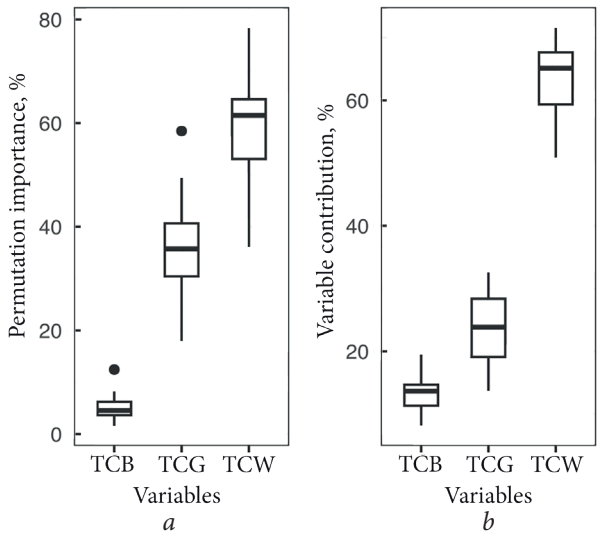

Fig. 4. Boxplots of permutation importance values (*a*) and variable contribution values (*b*) obtained from 30 replicated Maxent runs

The jackknife test, the results of which are presented in Fig. 5, indicated that the variables TCG and TCW, when used in isolation, yield a similarly high level of training gain, suggesting that they are approximately equally informative for model construction. However, the lack of any notable decrease in gain when these variables are omitted suggests that they contribute little unique information. In contrast, TCB demonstrated the lowest usefulness for model construction.

The final map, shown in Fig. 6, was obtained by reclas-

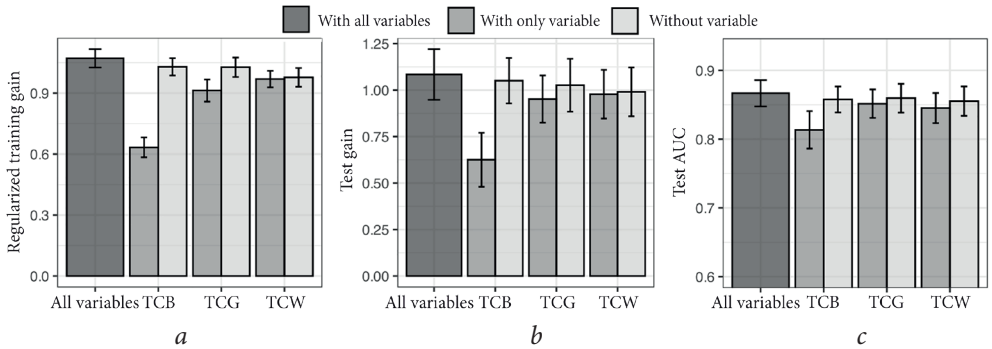

Fig. 5. Results of jackknife tests assessing the importance of environmental variables: *a* — regularized training gain; *b* — test gain; *c* — test AUC. The mean values from 30 Maxent runs are shown as bars, with ±1 SD represented by error bars

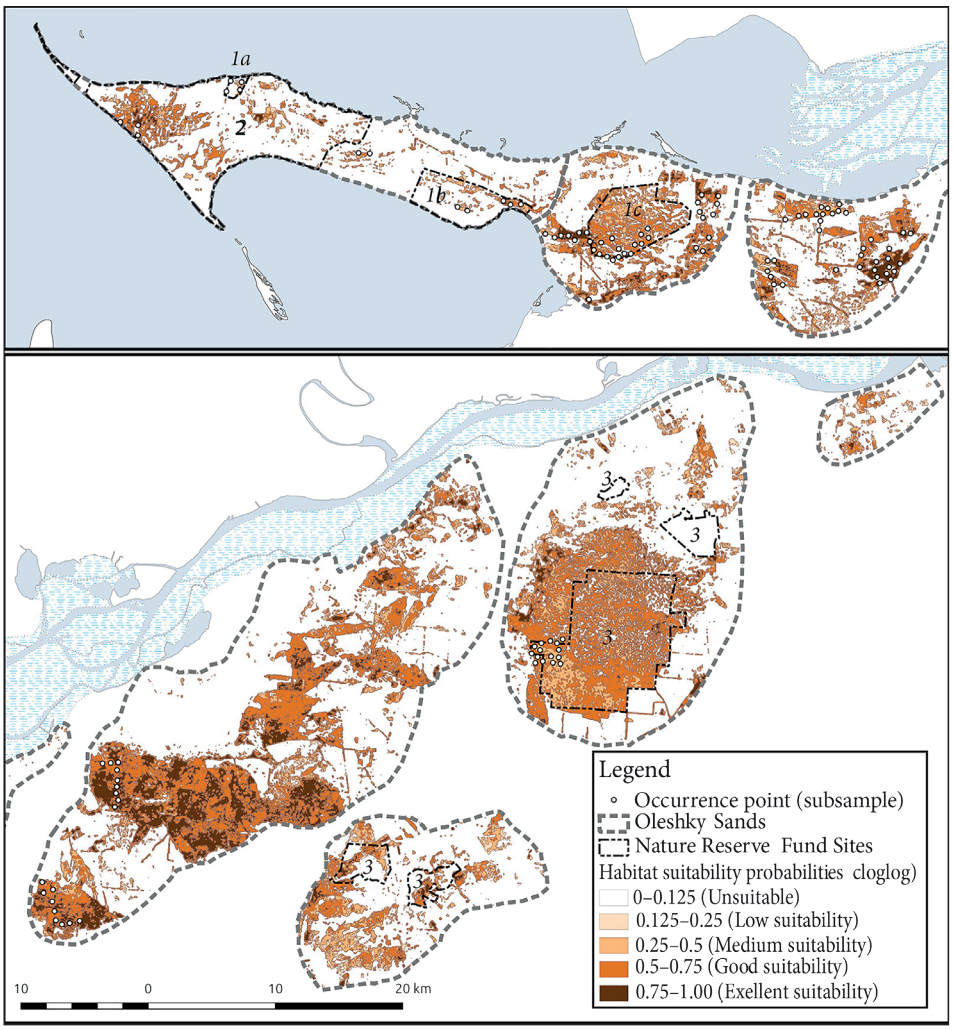

Fig. 6. Habitat suitability map for *S. t. falzfeini*. Nature Reserve Fund sites within the Oleshky Sands region: *1* — Black Sea Biosphere Reserve (sections: *1a* — Volyzhin Forest section; *1b* — Solonoozerna section; *1c* — Ivano-Rybalchanska section); *2* — Ivory Coast of Sviatoslav National Nature Park and Kinburn Spit Regional Landscape Park; *3* — Oleshky Sands National Nature Park

Table 3. **Habitat areas classified by suitability probability for *S. t. falzfeini* within the OS**

Arenas of OS	Classes of habitat suitability probabilities										Total	
	0–0.125 Unsuitable		0.125–0.25 Low Suitability		0.25–0.50 Medium Suitability		0.50–0.75 Good Suitability		0.75–1 Excellent Suitability			
	ha	%	ha	%	ha	%	ha	%	ha	%	ha	%
Kakhovska	3314	78.4	335	7.9	324	7.7	204	4.8	50	1.2	4227	100
Kozachelaherska	23507	56.8	2233	5.4	5439	13.2	9103	22.0	1080	2.6	41362	100
Oleshkyvska	34891	58.7	2462	4.1	3904	6.6	9998	16.8	8239	13.8	59493	100
Chalbaska	11398	65.6	1303	7.5	2166	12.5	1981	11.4	522	3.0	17371	100
Zburivska	9483	63.7	1172	7.9	1369	9.2	1836	12.3	1027	6.9	14887	100
Ivanivska	7914	55.3	906	6.3	2102	14.7	2596	18.1	796	5.6	14315	100
Kinburn Peninsula	17455	80.8	1070	4.9	1524	7.1	1258	5.8	295	1.4	21601	100
Total:	107962	62.3	9481	5.5	16828	9.7	26976	15.6	12009	6.9	173256	100

sifying the median map of habitat suitability generated by Maxent into five classes: class 1 (0–0.125) — Unsuitable, class 2 (0.125–0.25) — Low Suitability, class 3 (0.25–0.50) — Medium Suitability, class 4 (0.50–0.75) — Good Suitability, and class 5 (0.75–1) — Excellent Suitability. For each class of habitat suitability, the area was calculated individually for each arena, and the summarized results are provided in Table 3.

Discussion

In our study, we have developed a model that enables to estimate the distribution of potentially suitable habitats for *S. t. falzfeini* within the OS. The performance evaluation demonstrated the model's reasonably accurate predictive capabilities. This allows for an analysis of the spatial distribution patterns of *S. t. falzfeini* and the identification of key natural and anthropogenic factors driving its distribution. Furthermore, it provides a foundation for outlining some hypotheses regarding the impact of temporal dynamics of these factors on the population of the studied species.

One of the main habitat characteristics determining the habitat selection of *S. telum* in the western and northern parts of its range is the fraction of vegetation cover (Shenbrot et al., 1995). For example, at the northern border of its range *S. telum* prefers areas with 25–30% grass cover and does not occupy habitats with grass cover above 40% (Khodashova, 1953). Our studies have indicated that in the OS *S. t. falzfeini* also exclusively prefers areas with the sparse grass cover.

All geospatial environmental variables selected as proxies for modelling the spatial distribution of *S. t. falzfeini* reflect, to some extent, the spatial heterogeneity of the vegetation cover within the OS, albeit in different physical ways. For instance, it is well established that TCG correlates with vegetation parameters such as vegetation fractional cover, fresh biomass, and leaf area index. This correlation arises from TCG's response to the combination of high absorption in the visible spectrum (due to plant pigments and particularly chlorophyll) and high reflectance in the near-in-

frared spectrum (due to the internal leaf structure and the resultant scattering of near-infrared radiation), which is inherent in green vegetation (Crist & Cicone, 1984). The next geospatial variable, TCB, correlates with the total reflectance coefficient and reflects the physical processes that affect this coefficient (Vorovencii, 2007). The value of this variable increases with the thinning of vegetation (up to its complete absence) and with a decrease in soil humus content, reaching its highest values on bare sandy soils (Yousuf & AL-Khakani, 2021). Finally, TCW is determined by soil and vegetation moisture content (Crist & Cicone, 1984).

To better understand how the selected geospatial variables influence the spatial distribution of *S. t. falzfeini*, we closely examined their response curves (Fig. 3) while simultaneously analysing their spatial variation across the OS landscapes, comparing it with vegetation patterns observed in Sentinel-2 RSD imagery (using band combinations 12-8-3 and 8-4-3) within the QGIS software. As shown by the response curve for TCB (Fig. 3, *a*), areas with the lowest values of this variable are unsuitable for jerboa. As TCB increases beyond 0.2, the cloglog output rises exponentially, reaching its peak at around 0.65, after which it begins to decline. This decline is accompanied by increasing standard deviation values, indicating substantial variability in habitat suitability across areas with high TCB values. This can be explained by the fact that, within the OS, the highest TCB values are typical of both elevated areas with very sparse vegetation and low-humus soils, which are suitable for the jerboa, and dry lakebeds with light sandy substrates, which are unsuitable.

Response curve for TCG (Fig. 3, *b*) shows very low variability, and its shape indicates that complitely unsuitable conditions for *S. t. falzfeini* occur at both extremes of the gradient of this variable within the OS. Moreover, the elongated shape of the curve suggests that only a very narrow range of TCG values is suitable for *S. t. falzfeini*. Areas with TCG values below –0.03 are entirely unsuitable for the jerboa, as such values are typical of water bodies. Likewise, areas with TCG values above 0.03 are also unsuitable, as the vegetation there is either too dense (in the case of herbaceous communities) or consists of forest cover.

The left slope of the response curve for TCW (Fig. 3, *c*) lies entirely within the suitable habitat range, although the standard deviation values reveal considerable variability in the cloglog output across this portion of the curve, particularly in areas with TCW values below 0.27. Overall, TCW values along the left slope of the response curve (i. e., below –0.20) correspond to areas within the OS characterised by extremely sparse vegetation or, in some cases, by its near-complete absence (in which case TCW values fall below 0.27). Such areas are found almost exclusively on the Kozachelaherska Arena and, to a significantly lesser extent, on the Oleshkyvska Arena, while areas of any appreciable size with TCW values below 0.27 occur solely within the Kozachelaherska Arena. For TCW values greater than –0.20 (i. e., on the right slope of the curve), cloglog output values decrease, reaching zero at approximately –0.025. As TCW values increase within this range, vegetation cover becomes visibly denser. Areas with TCW values above –0.025 correspond to meadow, wetland, or forest vegetation, or open water bodies, and are entirely unsuitable for *S. t. falzfeini*.

Analysis of the habitat suitability map generated during the modelling process indicated that a substantial portion of the OS is unsuitable for *S. t. falzfeini*. An as-

Fig. 7. A burrow of *S. t. falzfeini* in natural sparse sandy-steppe vegetation (Ivanivska arena of OS, Ivano-Rybalchanska section of the Black Sea Biosphere Reserve, 5 May 2009)

Fig. 8. A burrow of *S. t. falzfeini* in a site with sandy vegetation at an early stage of regenerative succession following anthropogenic transformation (Kozachelaherska arena of OS, 12 October 2017)

Fig. 9. A burrow of *S. t. falzfeini* in a site with sandy vegetation regenerating on a burnt area that replaced a closed artificial pine forest following a large-scale fire in August 2007. A row of stumps near the burrow indicates that a forest once stood here (Oleshkyvska arena of OS, 26 May 2017)

sessment of habitat extent across the suitability classes (see Table 3) showed that approximately three-fifths of the OS area is entirely unsuitable for the species. In specific arenas, this proportion ranges from 55.3% to 65.6%, reaching as high as 78.4% in the Kakhovska arena and 80.8% on the Kinburn Peninsula.

We compared the distribution of habitats with different degrees of suitability for *S. t. falzfeini* with the distribution of various plant communities within the OS. It was observed that in all arenas, the largest area of unsuitable territories is represented by artificial pine plantations and, to a lesser extent, grassy associations that formed in relatively favorable hydroedaphic conditions and exhibited a higher fraction of vegetation cover. Due to the prevalence of such associations on the Kinburn Peninsula and the extensive presence of lakes within its borders, the proportion of habitats suitable for *S. t. falzfeini* on this peninsula is considerably lower compared to other arenas. As for the Kakhovska arena, the substantial share of unsuitable habitats is largely due to the fact that nearly half of its area is covered by built-up areas.

The habitats suitable for *S. t. falzfeini* primarily consist of elevated areas within the OS, characterized by sparse sandy-steppe vegetation associations that have developed due to limited soil moisture. These suitable habitats can include both primary natural plant associations, such as those found in the wood-steppe sections of the Black Sea Biosphere Reserve (Fig. 7), and associations at various stages of restorative succession following graz-

ing disturbances (Fig. 8). They are also represented in areas where sparse psammophilous steppe vegetation is regenerating following the destruction of artificial pine plantations by fire (Fig. 9). Additionally, areas with suitable conditions for *S. t. falzfeini* are those where vegetation density is maintained at an appropriate level through cattle grazing. However, such sites are scarce within the OS due to decline of cattle breeding in the region in last decades.

It is important to note that the extensive network of unsuitable areas greatly fragments the habitats of *S. t. falzfeini*, creating isolated patches of varying sizes and leading to the separation of the species population into distinct subpopulations. These isolated patches of potentially suitable habitats for *S. t. falzfeini* often include areas where the species is absent, as their size is insufficient to support isolated subpopulations. As a result, the fragmentation of habitats in the OS significantly reduces the overall habitat area for *S. t. falzfeini*, restricts gene flow, and has a negative impact on the overall population status, thereby increasing the risk of extinction for this subspecies.

When examining the distribution of suitable habitats for *S. t. falzfeini* in terms of land use, the largest area is located within forest fund lands. These areas are inherently vulnerable due to the ongoing threat of afforestation with artificial plantations, which has long been regarded as one of the most significant negative factors affecting *S. t. falzfeini* populations (Hyzenko 1985; Selyunina 2009). A further portion of suitable habitats falls within lands administered by rural territorial communities, where they are also under threat due to the common practice of allocating such areas for farming activities. Only the habitats situated within Nature Reserve Fund lands can be considered protected. Among these, the most important site for the conservation of *S. t. falzfeini* is the Black Sea Biosphere Reserve, as it preserves habitats in their natural condition.

Conclusions

The results obtained open up new opportunities for the study of *S. t. falzfeini*. The successful modelling of the species' spatial distribution using selected, temporally comparable satellite-derived metrics enables a retrospective analysis of changes in the distribution of *S. t. falzfeini* within the Oleshkyvski Sands, followed by a detailed evaluation of the factors that have influenced these changes over recent decades. Furthermore, the collected dataset of *S. t. falzfeini* burrow occurrence points and the model based on it capture the pre-war state of the jerboa population and may serve as a baseline for future assessments of the impacts of the occupation and military actions on this population.

Acknowledgements. I extend my sincere gratitude to Zoya Selyunina, Daria Korolesova, and Serhii Pliushch for their assistance in field data collection.

This research was carried out within the framework of the scientific projects "Conservation of populations of plant and animal species listed in the Red Data Book of Ukraine under the conditions of the Black Sea Biosphere Reserve and adjacent territories" (state registration number 0115U001142), and "Monitoring the state of natural complexes of the Black Sea Biosphere Reserve (Chronicle of Nature) in 2021–2025" (state registration number 0121U109174).

Supplementary materials. Supplementary materials for this article are available on the Zenodo repository at https://doi.org/10.5281/zenodo.15389095. They include a dataset of *S. t. falzfeini* burrow occurrence coordinates formatted according to the Darwin Core Standard; full-resolution georeferenced habitat suitability models for *S. t. falzfeini* (both as Maxent cloglog output and as a reclassified suitability map) in GeoTIFF format with a spatial resolution of 30 m/pixel; and Fig. 6 in high resolution. In addition, the repository contains JavaScript and bash scripts used for the preparation of the RSD.

REFERENCES

Abdelaal, M., Fois, M., Fenu, G. & Bacchetta, G. 2019. Using MaxEnt modeling to predict the potential distribution of the endemic plant Rosa arabica Crép. in Egypt. *Ecological Informatics*, **50**, 68–75. https://doi.org/10.1016/j.ecoinf.2019.01.003.

Aiello-Lammens, M. E., Boria, R. A., Radosavljevic, A., Vilela, B. & Anderson, R. P. 2015. spThin: an R package for spatial thinning of species occurrence records for use in ecological niche models. *Ecography*, **38** (5), 541–545. https://doi.org/10.1111/ecog.01132.

Araújo, M. B., Pearson, R. G., Thuiller, W. & Erhard, M. 2005. Validation of species–climate impact models under climate change. *Global Change Biology*, **11** (9), 1504–1513. https://doi.org/10.1111/j.1365-2486.2005.01000.x.

Araújo, M. B., Anderson, R. P., Márcia Barbosa, A., et al. 2019. Standards for distribution models in biodiversity assessments. *Science Advances*, **5** (1), eaat4858. https://doi.org/10.1126/sciadv.aat4858.

Baig, M. H. A., Zhang, L., Shuai, T. & Tong, Q. 2014. Derivation of a tasselled cap transformation based on Landsat 8 at-satellite reflectance. *Remote Sensing Letters*, **5** (5), 423–431. https://doi.org/10.1080/2150704X.2014.915434.

Bertoldi, G., Notarnicola, C., Leitinger, G., et al. 2010. Topographical and ecohydrological controls on land surface temperature in an alpine catchment. *Ecohydrology*, **3** (2), 189–204. https://doi.org/10.1002/eco.129.

Boria, R. A., Olson, L. E., Goodman, S. M. & Anderson, R. P. 2014. Spatial filtering to reduce sampling bias can improve the performance of ecological niche models. *Ecological Modelling*, **275**, 73–77. https://doi.org/10.1016/j.ecolmodel.2013.12.012.

Chandra, A. M. & Ghosh, S. K. 2007. *Remote sensing and geographical information system*. Repr., Alpha Science Intern, Oxford, 1–298.

Cobos, M. E., Peterson, A. T., Barve, N. & Osorio-Olvera, L. 2019. kuenm: an R package for detailed development of ecological niche models using Maxent. *PeerJ 7:e6281. https://doi.org/10.7717/peerj.6281.*

Crist, E. P. & Cicone, R. C. 1984. A Physically-Based Transformation of Thematic Mapper Data — The TM Tasseled Cap. *IEEE Transactions on Geoscience and Remote Sensing*, **GE-22** (3), 256–263. https://doi.org/10.1109/TGRS.1984.350619.

Franklin, J. & Miller, J. A. 2010. *Mapping species distributions*. Cambridge University Press. 1–320. https://doi.org/10.1017/CBO9780511810602.

GDAL/OGR contributors 2017. *GDAL/OGR Geospatial Data Abstraction software Library*. Open Source Geospatial Foundation. Available from: https://gdal.org.

Gitelson, A. A., Kaufman, Y. J., Stark, R. & Rundquist, D. 2002. Novel algorithms for remote estimation of vegetation fraction. *Remote Sensing of Environment*, **80** (1), 76–87. https://doi.org/10.1016/S0034-4257(01)00289-9.

Gorelick, N., Hancher, M., Dixon, M., Ilyushchenko, S., Thau, D. & Moore, R. 2017. Google Earth Engine: Planetary-scale geospatial analysis for everyone. *Big Remotely Sensed Data: tools, applications and experiences*, **202**, 18–27. https://doi.org/10.1016/j.rse.2017.06.031.

Gordienko, I. I. 1969. *Oleshkye Sands and biocoenotical relations in the process of their overgrowing*. Naukova Dumka, Kiev, 1–242 [In Russian].

Gromov, I. M. & Baranova, V. I., eds. 1981. *Catalogue of mammals of the USSR (Pleiocene-our days)*. Nauka, Leningrad, 1–456 [In Russian].

Hyzenko, A. I. 1985. On the abundance of the sand mole rat and the thick-tailed three-toed jerboa in Ukraine. *Vestnik zoologii*, No 1: 84–85 [In Russian].

Khodashova, K. S. 1953. Life forms of rodents of plain Kazakhstan and some patterns of their geographic distribution. *In*: *Transactions of the Institute of Geography of Academy of Science of the USSR . Vol. 54, is. 1*. Moscow, 33–194 [in Russian].

Kolodezhna, V. V., Vasyliuk, O. V. eds. 2025. *Destruction of the Kakhovka Reservoir: Environmental Consequences*. Druk Art, Chernivtsi, 1–112 [In Ukrainian].

Leyequien, E., Verrelst, J., Slot, M., Schaepman-Strub, G., Heitkönig, I. M. A. & Skidmore, A. 2007. Capturing the fugitive: Applying remote sensing to terrestrial animal distribution and diversity. *International Journal of Applied Earth Observation and Geoinformation*, **9** (1), 1–20. https://doi.org/10.1016/j.jag.2006.08.002.

Li, Z.-L., Tang, B.-H., Wu, H., et al. 2013. Satellite-derived land surface temperature: Current status and perspectives. *Remote Sensing of Environment*, **131**, 14–37. https://doi.org/10.1016/j.rse.2012.12.008.

Ministry of Environmental Protection and Natural Resources of Ukraine. 2020. Regulations on the National Nature Park "Oleshkyvski Pisky". Available from: https://mepr.gov.ua/documents/pro-zatverdzhennya-polozhennya-pro-natsionalnyj-pryrodnyj-park-Oleshkyvski-pisky/ [Accessed: 15 March 2025] [In Ukrainian].

Pearson, R. G. & Dawson, T. P. 2003. Predicting the impacts of climate change on the distribution of species: are bioclimate envelope models useful? *Global Ecology and Biogeography*, **12**(5), 361–371. https://doi.org/10.1046/j.1466-822X.2003.00042.x.

Phillips, S. J., Anderson, R. P. & Schapire, R. E. 2006. Maximum entropy modeling of species geographic distributions. *Ecological Modelling*, **190**(3), 231–259. https://doi.org/10.1016/j.ecolmodel.2005.03.026.

Phillips, S. J., Anderson, R. P., Dudík, M., Schapire, R. E. & Blair, M. E. 2017. Opening the black box: an open-source release of Maxent. *Ecography*, **40**(7), 887–893. https://doi.org/10.1111/ecog.03049.

Red Data Book of the Ukrainian SSR. 1980. Naukova Dumka, Kyiv, 1–504 [In Ukrainian].

Red Data Book of Ukraine. Animals. 1994. Shcherbak, M. M., ed. Kyiv, 1–464 [In Ukrainian].

Red Data Book of Ukraine. Animals. 2009. Akimov, I. A., ed. Kyiv, 1–600 [In Ukrainian].

Roberts, D. A., Dennison, P. E., Roth, K. L., Dudley, K. & Hulley, G. 2015. Relationships between dominant plant species, fractional cover and Land Surface Temperature in a Mediterranean ecosystem. *Remote Sensing of Environment*, **167**, 152–167. https://doi.org/10.1016/j.rse.2015.01.026.

Rusin, M. 2023. Phylogeography of the Western Populations of Stylodipus telum (Rodentia, Dipodidae) based on Mitochondrial DNA. *Zoodiversity*, **57** (1), 13–18. https://doi.org/10.15407/zoo2023.01.013.

Selyunina, Z. V. 1995. Jerboas (Dipodidea) of the Black Sea Biosphere Reserve region. *Nature Reserves in Ukraine*, 1, 23–28.

Shenbrot, G. I., Sokolov, V. E., Geptner, V. G. & Kovalskaya, Yu. M. 1995. *Dipodoidea. In: Mammals of Russia and adjacent regions.* Nauka, Moscow, 1–576 [In Russian].

Simoes, M., Romero-Alvarez, D., Nuñez-Penichet, C., Jiménez, L. & E. Cobos, M. 2020. General Theory and Good Practices in Ecological Niche Modeling: A Basic Guide. *Biodiversity Informatics*, **15** (2), 67–68. https://doi.org/10.17161/bi.v15i2.13376.

Tkachenko, V. S. 1999. These mysterious Oleshky Sands. *Zhyva Ukraina*, (3–4), 15–16 [In Ukrainian].

Tytar, V. M. 2011. The analysis of the species ranges: ecological-niche modeling-based approach. *Vestnik Zoologii*, *Supplement*, 5–93 [In Ukrainian].

Todd, S. W. & Hoffer, R. M. 1998. Responses of spectral indices to variations in vegetation cover and soil background. *Photogrammetric engineering and remote sensing*, **64** (9), 915–922.

Vorovencii, I. 2007. Use of the "Tasseled Cap" Transformation for the Interpretation of Satellite Images. *RevCad — Journal of Geodesy and Cadastre*, **7**, 75–82.

Yousuf, R. & AL-Khakani, E. 2021. Assessing Degree of Desertification Using Tasselled Cap Transformation and Spectral Indicators Techniques: Iraq. *Basic and Applied Sciences — Scientific Journal of King Faisal University*, **22** (1), 48–53.

Zagorodniuk, I. V. 2023. Priorities in nature conservation in times of war: the situation with the Great Meadow and the Great Steppe. *Visnyk Natsionalnoi akademii nauk Ukrainy*, 9, 12–23. https://doi.org/10.15407/visn2023.09.012 [In Ukrainian].

Zagorodniuk, I. & Korobchenko, M. 2023. Chorology of *Spalax arenarius*, an endemic rodent species of the Lower Dnipro Sands and Taurida steppe. *Theriologia Ukrainica*, **26**, 105–131. https://doi.org/10.53452/TU2611.

Received 25 May 2025
Accepted 22 April 2026